Available online at www.sciencedirect.com
SCIENCE DIRECT
Cement & Concrete Composites 28 (2006) 589–597
Cement & Concrete Composites
www.elsevier.com/locate/cemconcomp

A new approach for evaluating bond capacity of TRC strengthening

Regine Ortlepp [a,*], Uwe Hampel [b], Manfred Curbach [a]

[a] Dresden University of Technology, Department of Civil Engineering, Institut für Massivbau, D-01062 Dresden, Germany
[b] Dresden University of Technology, Department of Forest, Geo and Hydro Sciences, 01062 Dresden, Germany

Received 11 May 2006; accepted 12 May 2006
Available online 27 June 2006

Abstract

The anchoring of textile reinforced concrete strengthening layers (TRC-strengthening layers) for RC members has been studied with the help of double-lap-compression-tension-tests. Special difficulties are shown which differ from previously known strengthening materials like steel or FRP. For example, the non-linear material behaviour and the cracking of the TRC make it impossible to traditionally measure and analyse the deformation data by means of strain gauges in previously set and constant interval limits. An alternative method for logging and preparing measurement data with the help of the digital photogrammetry is illustrated. The measuring of the crack pattern of the strengthening layer indicates a division of the bond length into an uncracked (state I) and a cracked (state II) range. A first model for ascertaining the load carrying capacity of the bond is presented which takes into account the ranges of state I and II. Further extensions, which are necessary, are pointed out.

Keywords: Textile; Reinforced concrete; Bond; Anchoring; Digital photogrammetry

1. Introduction

RC members, of whom the load carrying capacity should be improved, have been strengthened by means of an additionally applied steel reinforced shotcrete for many years. Thereby, the textile reinforced concrete (TRC) represents a relatively new development in the field of strengthening and retrofitting. Instead of the traditional steel reinforcement, textile fabrics are used as reinforcing material for TRC. These fabrics are made of endless fibres, which can be interwoven with each other or sewn together by means of a stitching fibre. Depending on the application, different chemical fibres, e.g. alkali resistant glass fibres, carbon fibres or polypropylene fibres are used as fibre materials [1,2]. A high performance fine grained concrete with a maximum aggregate size of 1 mm is used as matrix.

Compared to a steel reinforced shotcrete strengthening, the textile reinforced concrete offers great advantages. Since the non-metallic fibres do not rust, the traditional concrete cover for protecting the reinforcement is not necessary anymore. This makes the application of extremely thin concrete strengthening layers of about 1 cm possible (Fig. 1) which on the one hand limits the increase of the dead load due to the strengthening and on the other hand maintains the geometric dimensions of the structural member as much as possible. Slabs and beams in bending [3] as well as beams and T-beams in shear [4] can be strengthened primarily, whereas partly a considerable increase of the load carrying capacity has been observed.

For the development of cross sectional models to design the strengthening of RC members, knowledge about the bearable tension force in the textile reinforced strengthening layer and about its deformation behaviour is necessary. The load transfer into the strengthening layer and its anchoring are also of special interest as illustrated in Fig. 2 (top) for the case of flexural strengthening. This problem is also of great significance for other forms of

* Corresponding author. Tel.: +49 (0)351/463 35304; fax: +49 (0)351/463 37289.
E-mail address: Regine.Ortlepp@tu-dresden.de (R. Ortlepp).

0958-9465/$ - see front matter © 2006 Elsevier Ltd. All rights reserved.
doi:10.1016/j.cemconcomp.2006.05.003

Fig. 1. Example of textile reinforced concrete.

strengthening, e.g. the shear strengthening of T-beams, because in this case the strengthening layer does not reach the compression zone (Fig. 2, right). The question arises if the anchorage in the beam web is sufficient in order to safely transfer tensile loads from the textile reinforced strengthening layer to the concrete substrate (here called old concrete). The problem of force transfer from the textile reinforced strengthening layer into the old concrete is studied on separate bond specimens. Special difficulties during the logging of measurement data in the bond tests and during the analysis of the results arise from the material properties of the textile reinforced concrete. Effects like the cracking of the strengthening layer in the bond length and the gradual change of the condition of the TRC from the uncracked to the cracked state have to be taken into account.

So far, no model is known to the authors for the calculation of the load carrying capacity for the bond of this material. A model for calculating the load carrying capacity of the bond for pure shear loading considering the non-linear material behaviour of the TRC is derived next. Additional special effects of the anchoring of the TRC strengthening material are pointed out and necessary model extensions are shown.

2. Special phenomena in TRC bond tests

2.1. Test setup

Conventional strengthening materials like steel, CFRP and GFRP show a linear stress–strain-behaviour in the application area. In opposition to that, the TRC shows a non-linear stress–strain-behaviour. According to Jesse [2] it can be approximately described as a tri-linear function. The cracking of reinforced concrete and the resulting change from state I to state II are prerequisites for an effective use of TRC. Because of its non-linear material behaviour, TRC-strengthening layers must be more compared

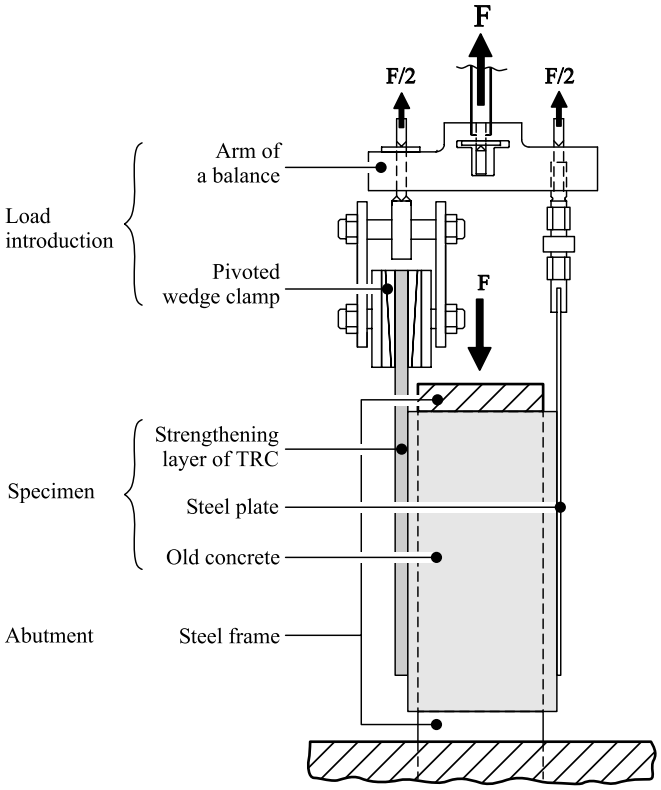

Fig. 3. Schematic illustration of the test setup.

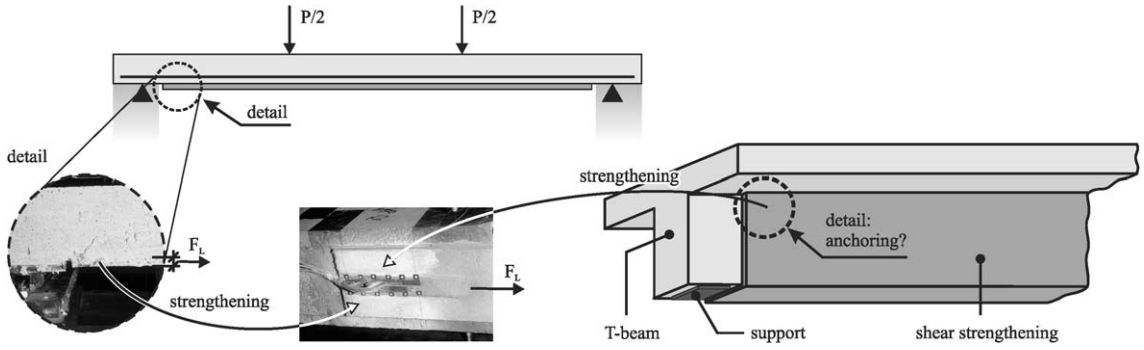

Fig. 2. Anchoring problem of flexural and shear strengthening.

with shotcrete or ferrocement [5] than with FRP-Products. Specific needs in the test setup and the deformation measurement result from this. In the context of the Collaborative Research Centre 528 at Dresden, a test setup was developed which may take the individual properties of the TRC into consideration (Fig. 3). A double-lap-compression-tension-specimen was selected.

As has been mentioned, cracking of the textile reinforced concrete takes place. This would not occur simultaneously in two TRC strengthening layers within a given time. The formation of cracks within the TRC strengthening layer results in a sudden change in length and an unloading of the strengthening layer in a kind of displacement-controlled test. Thus, the opposite strengthening layer would momentarily be loaded by impulse that might cause the specimen to begin to oscillate from one side to the other. For this reason, two strengthening layers of different materials and cross sections are chosen. Besides the TRC strengthening layer that is laminated and to be analysed, a steel plate is glued on the other side of the old concrete substrate. An arm of balance construction will guarantee the equal force distribution to both strengthening layers. Refs. [6,7] can be consulted for a detailed description of the test setup.

2.2. Special phenomena of TRC bond

Fig. 4 schematically shows a section of the specimen of Fig. 3 during the bond test. Only half of the specimen with the TRC strengthening layer is displayed in the figure. In the course of the bond test, cracks develop at first along the free length of the strengthening layer with increasing tension load, when the tensile strength of the fine-grained concrete is exceeded in this area. Then transversal cracks, starting from the loaded end of the bond length occur at the side surfaces of the TRC strengthening layer. A dramatic increase in crack formation is typical just before the ultimate load is attained. A horizontal bond crack develops as clearly visible in Fig. 4, from which transversal cracks develop. This horizontal crack forms the cross sectional area of the break in the case of a bond failure.

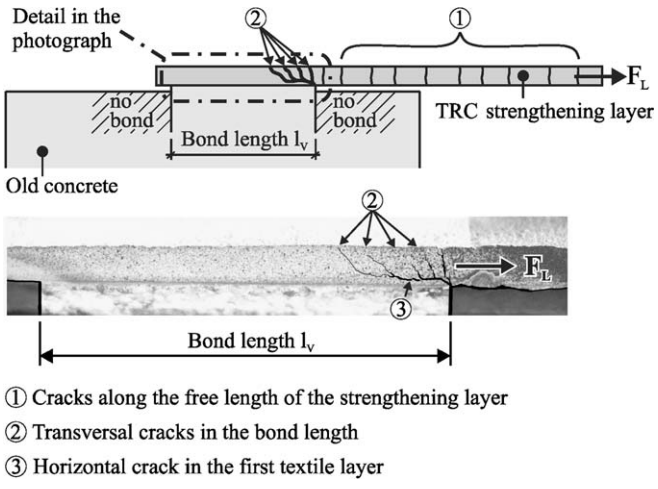

Fig. 4. Schematic illustration of cracking.

Due to the cracking, one further peculiarity of the TRC strengthening material arises: as opposed to the currently known strengthening materials, steel and FRP whose strain behaviour is equivalent to a continually increasing function the cracks in TRC result in discontinuities in the strain distribution. Consequently, the formation of single cracks drastically affects the distribution of the deformation so that a traditional deformation measurement, e.g. with the use of strain gauges or LVDT in previously set interval limits, cannot be carried out in the case of TRC. This problem has been discussed in detail in [6].

On this account, a reasonable measurement data logging is only feasible by means of a method that includes the developing crack pattern. With the help of digital photogrammetry, uninterrupted scanning of the bond length can be done. This method provides the distribution of the deformation in the bond length, which includes the crack opening width and the position of the individual cracks.

3. Experimental measurement

The bond behaviour of TRC strengthening layers with the old concrete is investigated by way of experiments. These experimental investigations are composed of the logging of the crack angle from the bond test on the one hand and the deformation measurement during the bond test by means of digital photogrammetry on the other hand.

3.1. Analysis of crack angles in the bond length

Previous investigations showed that the crack angles in the strengthening layer have also an enormous influence on the shear load bearing properties [7]. For this reason, their distribution along the bond length has been analyzed more precisely. First of all the cracks on the side surfaces of the strengthening layer were made visible on the prevarnished surface using black ink. Next, the crack pattern was digitally photographed head-on, i.e. without distortion, on both side surfaces of the strengthening layer. The cracks were gauged from the obtained image data (Fig. 5). The received data of the crack angles have been numerically analyzed depending on their position in the bond length (Fig. 6). From this a crack angle relationship of the bond length is obtained for every test series by means

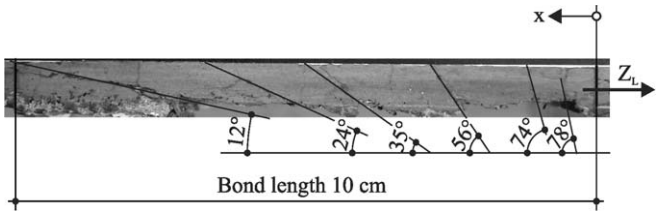

Fig. 5. Crack pattern of a strengthening layer in the bond length with dimensioning.

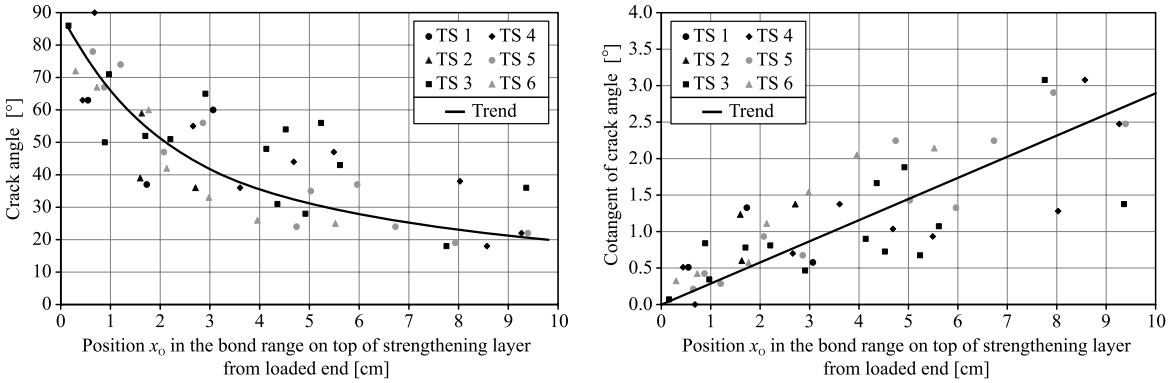

Fig. 6. Result of the analysis of the crack pattern of one test series.

of a statistical analysis. This relationship can be used for further evaluating the respective test series.

The plot of the cotangent of the crack angle over the crack position x_o in the bond length can be approximated by a simple linear relationship (Fig. 6).

3.2. Application of digital photogrammetry for measuring deformations and cracks

Methods of digital photogrammetry are suitable for the automatic measurement of two and three-dimensional displacements fields, deformations and surface defects such as cracks of test objects and structures during short and long term load tests [8–10].

Bond tests were carried out in order to measure and detect the crack positions and crack widths during the load test. Fig. 7 shows the configuration of the digital photogrammetry system, which was used, relying on two digital cameras and mirrors. The mirrors allow the image acquisition of the front and the sides of the test specimen simultaneously.

The sensor of the digital camera in use (Kodak Megaplus) is a CCD with $2k \times 2k$ Pixel (1–2 Hz), a fillfactor of 100% and a radiometric resolution of 10 bits. High precision measurements can be done with this type of camera. The methods of the developed digital photogrammetry system show a precision of up to 1/50 pixel for natural textures and up to 1/100 pixel for artificial signalizations [9,10]. This precision is necessary to detect deformations of up to 1 μm and crack widths of up to 3 μm in a measurement area of $\approx 100\ \text{mm} \times 100\ \text{mm}$. Fig. 8 shows only one profile of the relative displacements in the tension-direction. The term profile means a load-aligned line for evaluating photogrammetric data, see Fig. 9. The in-plane displacements show a significant number of cracks.

Fig. 9 shows the result of the crack detection for the whole measurement area near failure. The branching of cracks can be a problem if the measurement profile is crossing near it. In order to reduce this influence, the operators have to choose the position of the profiles immediately. The crack analysis modules calculate the crack position and crack width for all load images. The results for one profile are shown in Fig. 10.

Further investigation is needed to implement adaptive methods to develop a fully automatic module for the crack analysis of profiles or even of the whole measurement area.

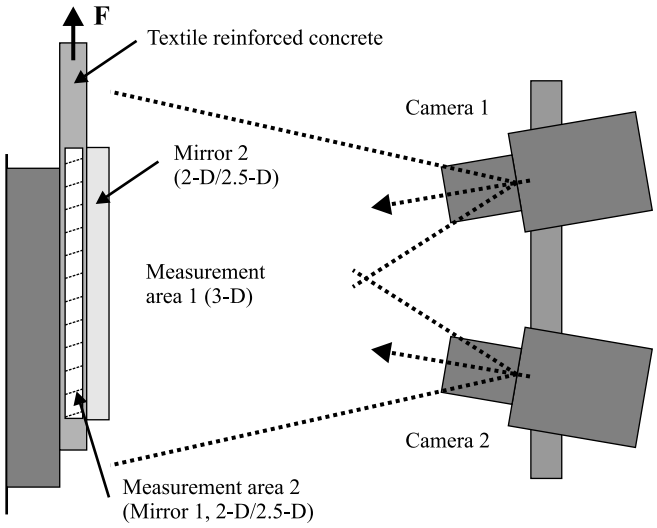

Fig. 7. Configuration of the digital photogrammetry system.

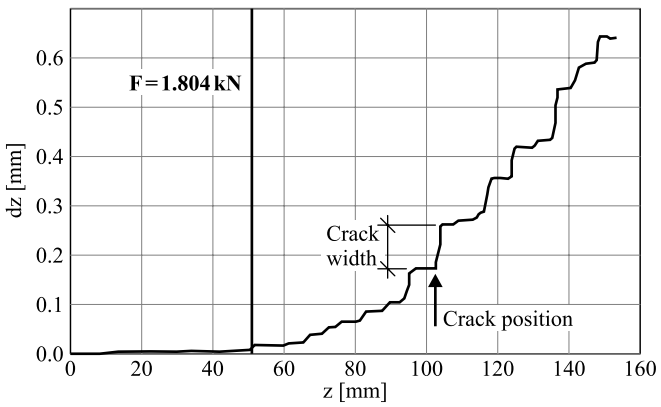

Fig. 8. Result of deformation analysis in tension direction.

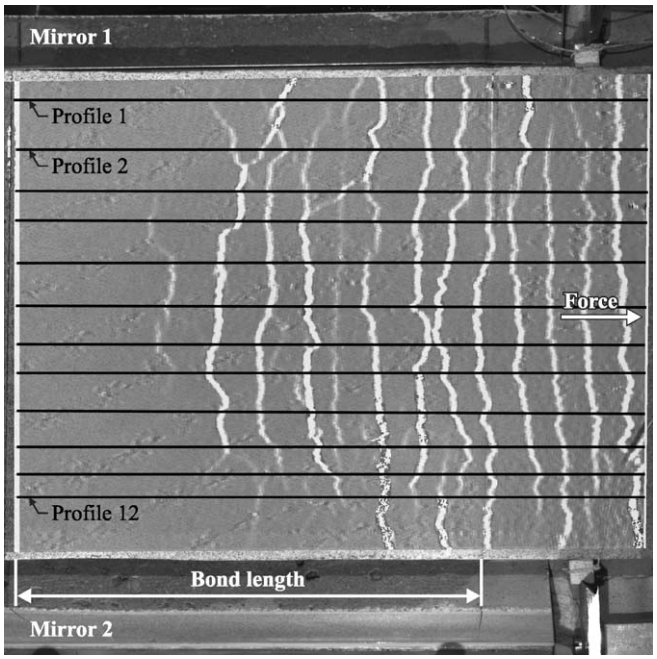

Fig. 9. Result of crack analysis for one load image near the break.

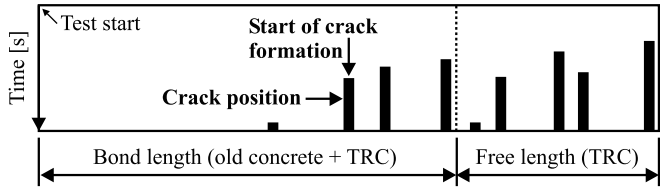

Fig. 10. Results of crack analysis for one profile in tension direction.

3.3. Analysis of deformation data

The measurement by means of the digital photogrammetry provides data for the relative displacement (slip) in the bond length over several load levels (Fig. 11) for each measuring profile that has been preselected (Fig. 9). Using these data, further analysis is carried out by way of defining intervals—in which a mean strain can be calculated—by adapting them to the crack pattern (so-called adaptive interval definition, see also [6,11]). The calculation is carried out separately for each measuring profile. Therefore, the intervals of each profile are defined depending on the existing crack pattern in such a way that one crack is located accurately between the interval limits [6]. Since the cracks are not straight, a different interval division arises for each of the several measuring profiles. Hence, the curves of the relative displacement (slip) over the bond length show in part significant differences. In order to obtain uniform information of the whole strengthening layer, the displacement data of all measuring profiles are considered. In this manner, an approximately smeared crack pattern over the whole width of the strengthening layer is gained. Hence, a smoother progression of the slip curves is achieved, which can be used for further evaluation. This has a particular effect on a very inhomogeneous crack pattern with many bifurcations. Fig. 12 shows schematically the distribution of the strain values after smoothing, which have been calculated from the relative displacement (slip), for selected load levels.

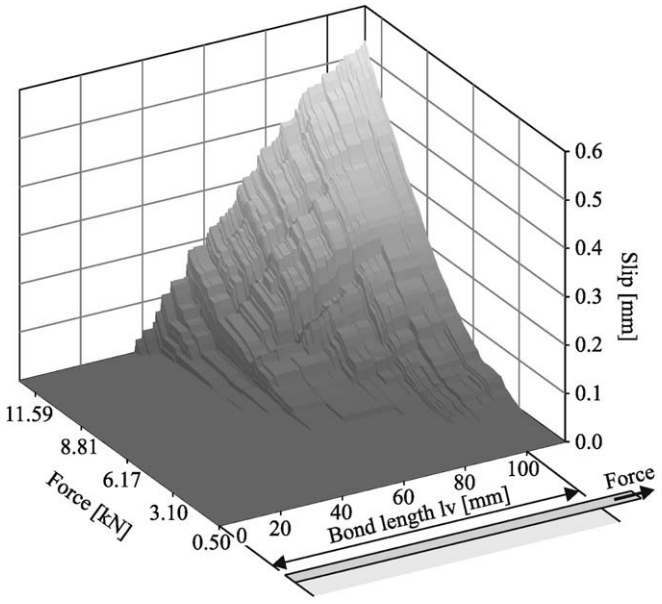

Fig. 11. Relative displacement (slip), measured on the top of the strengthening layer in the bond length over all load levels as average values of all measuring profiles.

As Fig. 12 shows, the strains run initially at low load levels, starting at the loaded end of the bond length and decreasing towards the unloaded end of the bond length. The rear part of the bond length that is the unloaded end, receives thereby almost no deformations. When the load increases, the strains increase at the beginning of the bond length, i.e. the loaded end, but fall steeply toward the mid part of the bond length. The rear part of the bond length still does not receive significant deformations. With further increase in load, a peculiarity of the TRC arises. A

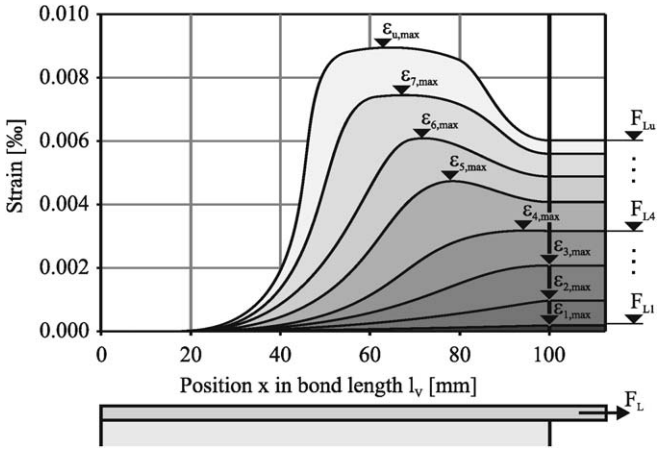

Fig. 12. Smoothed strains in the bond length for selected load levels, schematically.

maximum strain front starts to develop at the beginning of the bond length and moves backward into the bond length with increasing load. In comparison to this, the strain distribution of well-known strengthening materials like steel or FRP is characterized by a continuous decrease of the strain values over the bond length towards the unloaded end. This is caused by the linear material behaviour of these strengthening materials till bond failure.

According to Jesse [2] textile reinforced concrete shows a tri-linear material behaviour. When using this tri-linear stress–strain-relationship of the strengthening layer for evaluating stress from the measured strain, a not-monotonic stress distribution in the bond length arises as a result of the maximum strain front that is moving backward into the bond length. This stress distribution is characterised by a local maximum in the bond length; that is the stresses calculated from the strain initially rise beginning at the loaded end of the bond length. So we have calculative lower stress values at the loaded of the bond length then behind it. Some similar phenomenon has been observed in fibre pull-out [12]. In fact, the stress values should decrease up to the unloaded end because of stress transfer. Thus, it becomes obvious that no bond stresses can be calculated from such a stress distribution by means of the traditional algorithm of using stress differences [2] due to the material properties, because in this way negative bond stress values would result. Consequently, no bond–slip-relationship can be calculated for strengthening layers of textile reinforced concrete, as it is known from linear-elastic adhesive strengthening lamellas. As a result of the material behaviour, the essential prerequisites for the validity of the usual underlying assumptions—constant strain distribution over the thickness of the strengthening layer and slip occurs only in the adhesive joint—are not fulfilled.

The occurrence of the maximum strain into the bond length is consistent with a cumulative transversal cracking and a run of the bond crack into the bond length along the first textile layer facing the old concrete,. This is visible from recording of the side faces of the strengthening layer by means of the digital photogrammetry. It is characteristic that the rear part of the bond length shows no cracking up to the end of the loading and hardly undergoes deformations. The uninterrupted cracking in the front part of the bond length is followed by a sudden failure of the remaining rear part of the bond length in the ultimate limit state (ULS).

The formation of cracks, i.e. the change of the state of the TRC strengthening layer, in the bond length is schematically displayed in Fig. 13 versus a cumulative increase of the load level up to failure. At initial loading, the whole bond length l_V is initially uncracked, i.e. the whole bond length stands in state I. At a certain load level, the cracking in the bond length starts. When the cracking begins, the bond length divides into two parts: (a) a cracked part (state II) at the loaded end of the bond length and (b) an uncracked part (state I) at the unloaded end of the bond length (see Fig. 14). When the load is increased, the cracked

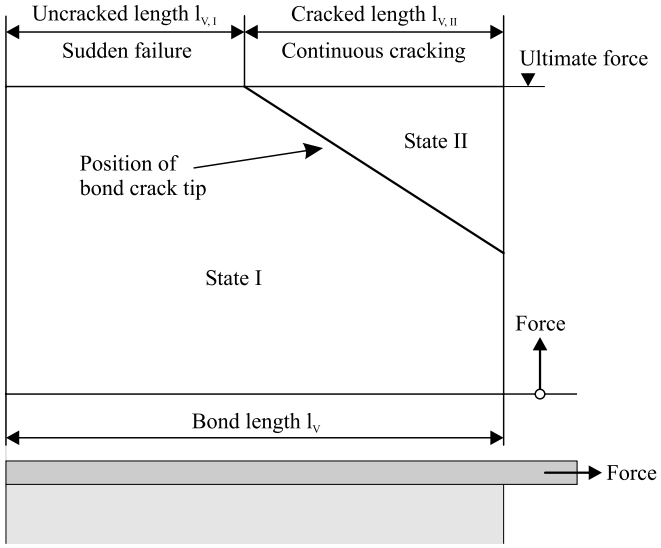

Fig. 13. Change of the ranges in state I + II in the bond length when increasing load level.

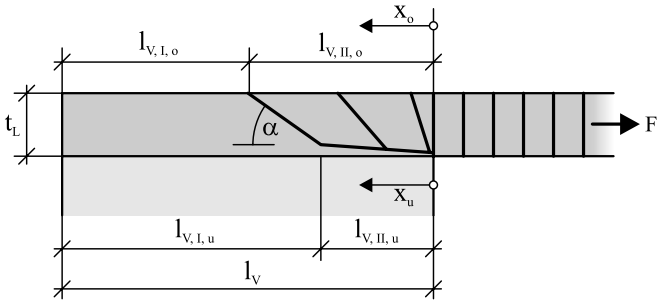

Fig. 14. Definition of symbols.

part of the bond length $l_{V,II}$ increases as well. This is accompanied by an uninterrupted bond cracking along the lowest layer of the textile reinforcement (see Fig. 4). The uncracked remainder part of the bond length $l_{V,I}$ is thereby equivalently shortened. When $l_{V,Iu}$ reaches a minimum value, a sudden failure occurs.

4. Model development

4.1. General remarks

The thickness of the strengthening layer t_L, the bond length l_V, the lengths of their parts in state I ($l_{V,I}$) and state II ($l_{V,II}$) on the top (subscript o) and on the bottom side (subscript u) of the strengthening layer as well as the crack angle α are displayed in Fig. 14.

The last transversal crack separates the cracked from the uncracked range of the bond length. The location of this point in the bond length occurs at a different position on the top and on the bottom side of the strengthening layer, because of the angle of this transversal crack. The measurement of the position of the crack by means of digital photogrammetry can only be done on the top side of the

strengthening layer, which means that, initially, the lengths $l_{V,I,o}$ and $l_{V,II,o}$ on the top side are found after the evaluation of the measured data from the test. However, the length ratio $l_{V,I,u}$ and $l_{V,II,u}$ at the bottom side of the strengthening layer are of interest for implementation into the model, because the bond crack develops in this area, from which the cross section at failure develops. For this reason, we have to differentiate between these two dimensions at first. The length ratio on the top side can be converted into the length ratio at the bottom side using the crack angle α and the thickness of the strengthening layer t_L.

4.2. Proposed model

The failure of a TRC strengthening layer bonded to an old concrete substrate can in principle take place in three different layers [6,13,14]: (1). delamination in the textile layer, (2) failure in the bond joint and (3) failure of the old concrete, whereby the second failure mode can be prevented by means of a sufficient surface pre-treatment (e.g. sandblasting).

Whether bond failure occurs in either one of the two extreme layers (TRC or old concrete), depends on the load carrying capacity of these two layers. The load carrying capacity of the old concrete is the crucial factor when a failure in the old concrete occurs while the load carrying capacity of the fine-grained concrete of the reinforcing textile is significant when failure in the textile layer appears. Results from previously done adhesive tensile tests have shown that only the remaining matrix between the fibres takes part in the load transfer through the textile layer [14]. The dimension of this effective area (Fig. 15) significantly affects the load carrying capacity in the textile layer. In ferrocement this area should exceed 70% [5].

The ratio of the effective area to the total area is expressed by the effective area ratio $k_{A,eff} = \frac{A_m}{A}$ (Fig. 15). This effective area ratio can be determined by area evaluation for each individual textile. Thus, the strength of the fine grained concrete in the strengthening layer, which is initially higher than the strength of the old concrete, is reduced by this factor $k_{A,eff}$. Consequently in which layer the bond failure occurs, depends on the effective area ratio of the textile reinforcement.

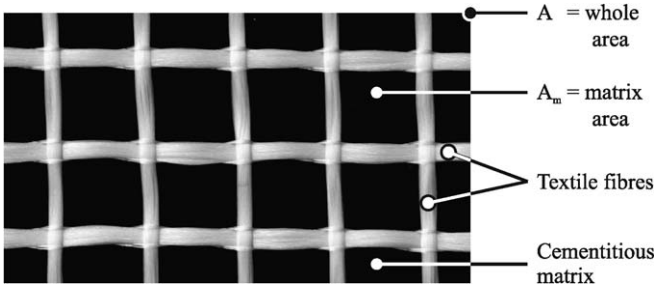

Fig. 15. Area ratios in a textile layer.

In addition to the pure bond failure modes specified above, a mixed failure mode can also occur. Thus, one part of the bond length fails due to a progressive formation of the bond crack because of delamination in the textile layer, whereby this part still participates in the load transfer by means of friction along the bond crack. The remainder of the bond length finally fails by disruption in the old concrete (Fig. 16). This failure mode has also to be considered for the development of a model.

As mentioned earlier, the geometric proportions on the bottom side of the strengthening layer are of particular interest for modelling the bond stress transfer, because the bond crack forms along the first textile layer facing the old concrete. Therefore, only the parts "cracked" and "uncracked" on the bottom side of the strengthening layer serving as reference level are considered in the subsequent modelling. In order to simplify this, a second subscript I and II is introduced to refer to states I (uncracked) and II (cracked) (Fig. 17). The maximum transferable bond force in the ULS is defined as $F_{L,Vu}$.

The ultimate bond force $F_{L,Vu}$ in the strengthening layer is transferred to the old concrete by means of bond stresses in both the cracked range ($l_{V,II}$) and the uncracked range ($l_{V,I}$). Thus, it is composed of a bond force component in the cracked range, which is transferred by the bond crack, and a bond force component in the uncracked remainder range of the bond length in the ULS (Eq. (1)).

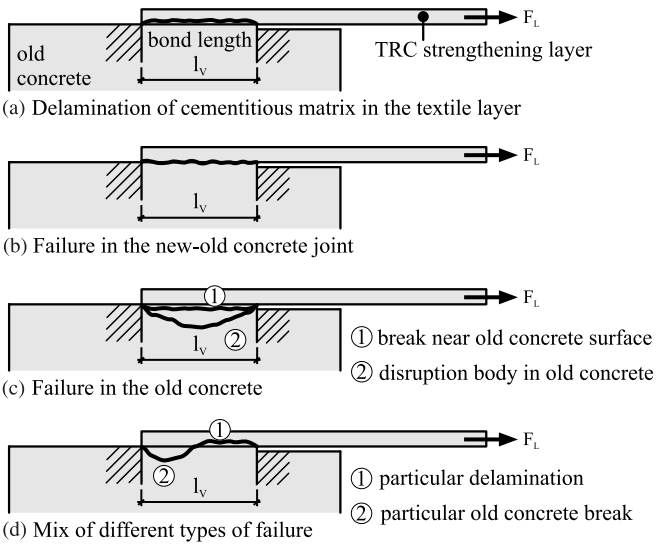

Fig. 16. Mixed bond failure, schematically.

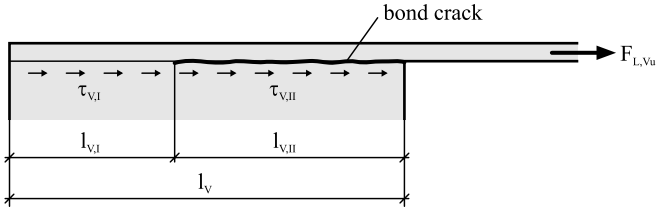

Fig. 17. Definition of symbols for the modelling.

$$F_{L,Vu} = b_L \times (l_{V,I} \times \tau_{Vu,I} + l_{V,II} \times \tau_{V,II}). \quad (1)$$

Where:

$F_{L,Vu}$ ... ultimate bond force,
b_L ... width of the strengthening layer,
$l_{V,I}$, $l_{V,II}$ ... length of the uncracked and cracked range of the bond length respectively,
$\tau_{Vu,I}$ ... ultimate bond stress (shear strength) in $l_{V,I}$ and
$\tau_{V,II}$ ... bond stress (shear stress) in $l_{V,II}$.

The failure along the bond crack takes place in the layer of the textile reinforcement. No uninterrupted formation of bond crack could be observed in the tests which were carried out. Therefore it will not be regarded as a possible failure layer in the model.

The bond stress $\tau_{V,II}$ along the layer of textile reinforcement refers to the total area of the bond crack. However the shear force is only transferred by the ratio of the fine grained concrete matrix between the fibres, thus an effective bond stress—to be transferred by crack friction—occurs in the bond crack in the textile reinforced fine grained concrete layer, landing to:

$$\tau_{V,II,fc} = \frac{\tau_{V,II}}{k_{A,eff}}. \quad (2)$$

In contrast to the cracked part of the bond length, we have to differentiate between two possibly different failure layers in the uncracked remainder part of the bond length $l_{V,I}$. The sudden failure of the remainder part can continue in the textile layer. In this case, the effective fine grained concrete area in the arising crack layer has to be considered, in just the same way as the bond crack described above. That means, the effective bond stress of the fine grained concrete in the ULS is conditioned—similar to the interrelation for the bond crack, indicated above—by the ultimate shear stress $\tau_{Vu,I}$ for the whole remainder area. Thus

$$\tau_{V,I,fcu} = \frac{\tau_{Vu,I}}{k_{A,eff}}. \quad (3)$$

Furthermore, the remainder part of the bond length which remains until failure in state I, can also fail in the old concrete subsurface. The old concrete itself is not disturbed by the textile reinforcement. Thus, the bond shear stress in the old concrete in the ULS is identical to the ultimate shear stress $\tau_{Vu,I}$ of the remainder area, which stayed in state I. Thus

$$\tau_{V,I,cu} = \tau_{Vu,I}. \quad (4)$$

As described above, the arising failure layer depends among other things on the effective area ratio $k_{A,eff}$ of the textile reinforcement. Thus, the smaller of the two ultimate shear stresses $\tau_{Vu,I}$, which result from the shear stress of the old concrete and the fine grained concrete in the textile layer respectively (Eq. (5)), controls the failure:

$$\tau_{Vu,I} = \min \begin{Bmatrix} \tau_{V,I,cu} \\ k_{A,eff} \times \tau_{V,I,fcu} \end{Bmatrix}. \quad (5)$$

The ultimate bond force $F_{L,Vu}$ from Eq. (1) can therefore be written as follows (Eq. (6)):

$$F_{L,Vu} = b_L \times \left(l_{V,I} \times \min \begin{Bmatrix} \tau_{V,I,cu} \\ k_{A,eff} \times \tau_{V,I,fcu} \end{Bmatrix} + l_{V,II} \times k_{A,eff} \times \tau_{V,II,fc} \right). \quad (6)$$

In this way, the maximum bearable force $F_{L,Vu}$ of a certain bond length l_V can be calculated from the shear stress, that is transferable by crack friction, and the ultimate shear stress of the old and fine grained concrete parallel to the bond joint respectively. The proposal for the model developed here assumes pure shear loading in the whole bond length.

5. Further work

A model was developed to calculate the ultimate transferable bond force $F_{L,Vu}$ for a given bond length l_V in terms of the transferable bond strength in the old concrete substrate and in the fine grade concrete (TRC layer). The model accommodates differences in the bond length in state II (cracked) and state I (uncracked). The model is applicable, assuming pure shear loading in the bond length. When the above model is compared to Strut-and-Tie-model for the bond length suggested in [14], then in addition to pure shear loading a lateral tension (peel-off) must be considered. Upgrading of the model developed in this study to account for the influence of the peel-off force is the aim of a future research.

Acknowledgements

The authors gratefully thank the German Research Foundation and their partners within the Collaborative Research Centre 528 "Textile Reinforcement for Structural Strengthening and Retrofitting" for their support.

References

[1] Hempel R, Franzke G, Curbach M, Offermann P. Improvement of the properties of concrete by means of textile reinforcements made of alkali resistant glass filament yarn. In: Proceedings of the12th International congress of the international glassfibre reinforced concrete association—CRC 2001, Dublin, Ireland, 14–16 May 2001. CD-ROM.
[2] Jesse F, Ortlepp R, Curbach M, Tensile stress–strain behaviour of textile reinforced concrete. In: IABSE, AIPC, IVBH, editors. Proceedings of the IABSE symposium, "Towards a better built environment—innovation, sustainability, information technology", Melbourne, Australia, September 2002—CD-ROM.
[3] Brueckner A, Ortlepp R, Curbach M. Textile reinforced concrete—applications and bond specifics. In: CEB-FIP, editor. Proceedings of the fib-symposium concrete Structures—the Challange of Creativity, Avignon, 26–28 April 2004. Book of Abstracts and CD-ROM. p. 162.
[4] Brueckner A, Ortlepp R, Curbach M. Textile reinforced concrete for strengthening in bending and shear. J Mater Struct 2006; 39, in press.
[5] Naaman AE. Ferrocement and laminated cementitious composites. Ann Arbor: Techno Press 3000; 2000.
[6] Ortlepp R, Curbach M. Bonding behaviour of textile reinforced concrete strengthening. In: Naaman AE, Reinhardt H-W, editors.

High performance fiber reinforced cement composites—HPFRCC 4', Proceedings of the fourth international RILEM workshop, Ann Arbor, USA, 15–18 June 2003. Bagneux: RILEM; 2003 (PRO 30). p. 517–27.

[7] Curbach M, Baumann L, Beyer R. Flächige Übertragung der Schubspannungen vom Altbeton in den textilbewehrten Beton. Two-dimensional shear stress transfer from old concrete to textile reinforced concrete. In: Curbach M, editor. Sonderforschungsbereich 528—Arbeits- und Ergebnisbericht für die Periode II/1999–I/2002. Dresden University of Technology; 2001. p. 207–46 [in German].

[8] Opitz H, Hampel U. Application of the digital photogrammetry in case of load testing in civil engineering. In: Anspruch und Tendenzen in der experimentellen Strukturmechanik, Gesa-Symposium 1999, VDI Berichte, vol. 1463, 6.–7.5; 1999. p. 311–6.

[9] Hampel U, Maas, H-G. Schubversuche an textilbewehrten Betonproben. Bond tests with textile reinforced concrete specimens. In: Luhmann T, editor. Nahbereichsphotogrammetrie in der Praxis—Beispiele und Problemlösungen. Heidelberg: Herbert Wichmann; 2002. p. 281–4 [in German].

[10] Hampel U, Maas H-G. Application of digital Photogrammetry for measuring deformation and cracks during load tests in civil engineering material testing. In: Grün A, Kahmen H, editors. Optical 3-D measurement techniques VI, vol. II; 2003. p. 80–8.

[11] Maas H-G, Hampel U, Schulze M. Photogrammetrische und computertomographische Erfassung von Deformationen, Rissentwicklungen und Strukturveränderungen bei Belastungsversuchen von textilverstärkten Probekörpern. Application of digital photogrammetry and computer tomography for measuring deformations, cracks and structural changes during load tests of textile reinforced test objects. In: Curbach M. editor. Textile reinforced structures: Proceedings of the second colloquium on textile reinforced structures—CTRS2, Dresden, Germany, 29 September—1 October 2003. Dresden University of Technology; 2004. p. 187–200 [in German].

[12] Naaman AE, Namur Jr G, Alwan J, Naim H. Fiber pull-out and bond slip. Part I: Analytical study. ASCE J Struct Eng 1991;117(9): 2769–90.

[13] Ortlepp R, Curbach M. Bond failure mechanisms of strengthening layers made of textile reinforced concrete. In: Proceedings of the 13th international congress of the international glassfibre reinforced concrete association—CRC 2003, Barcelona, Spain, 6–8 October 2003. Book of abstracts and CD-Rom.

[14] Ortlepp R, Ortlepp S, Curbach M. Stress Transfer in the bond joint of subsequently applied textile reinforced concrete strengthening. In: di Prisco M, Felicetti R, Plizzari GA. editors. Fibre-reinforced concretes: Proceedings of the sixth international RILEM-symposium—BEFIB 2004, Varenna, Italy, 20-22 September 2004. Bagneux: RILEM; 2004. p. 1483–94.